DOI: 10.63527/1607-8829-2025-1-60-80

S. Mamykin[1] (https://orcid.org/0000-0002-9427-324X),
B. Dzundza[2] (https://orcid.org/0000-0002-6657-5347),
R. Shneck[3] (https://orcid.org/0000-0002-5802-1352),
L. Vikhor[4] (https://orcid.org/0000-0002-8065-0526),
Z. Dashevsky[3] (https://orcid.org/0000-0001-9268-4873)

[1]V.E. Lashkaryov Institute of Semiconductor Physics, National Academy of Sciences of Ukraine, Kyiv, 03028, Ukraine;
[2]Department of Computer Technique, Vasyl Stefanyk Precarpathian National University, Ivano-Frankivsk, 76000, Ukraine;
[3]Department of Materials Engineering, Ben-Gurion University of the Negev, Beer-Sheva, 84105, Israel;
[4]Institute of Thermoelectricity of the NAS and MES of Ukraine, 1 Nauky str., Chernivtsi, 58029, Ukraine

Corresponding author: Z. Dashevsky, e-mail: *zdashev@bgu.ac.il*

Development of Solar Energy Systems Based on High Performance Bulk and Film Thermoelectric Modules

Due to the increase in energy demand and depletion of natural resources, the development of energy harvesting technologies becomes very important. Thermoelectric devices, based on the direct conversion of heat into electrical energy, are the essential part of cost-effective, environmentally friendly, and fuel-saving energy sources for power generation, temperature sensors, and thermal management. High reliability and long operation time of thermoelectric energy systems lead to their extensive use in space industry and gas pipe systems. Development and wide application of solar thermoelectric converters (generators) is mainly limited by relatively low thermoelectric conversion efficiency. In this work, we suggest for the first time to use direct conversion of solar energy by systems based on high-performance multistage thermoelectric modules operating in the temperature range of 300 – 900 K for creation of autonomous systems with electric power up to 500 W and electric efficiency up to 15 %. Furthermore, we have developed film thermoelectric modules on thin flexible substrates with the figure of merit corresponding to that of bulk modules. Such film thermoelectric converters with output voltage of several volts and electric power of several microwatts can be used in solar energy micro-systems.

Key words: solar energy, thermoelectric module, figure of merit, film thermoelectric micro-converter.

Citation: S. Mamykin, B. Dzundza, R. Shneck, L. Vikhor, Z. Dashevsky (2025). Development of Solar Energy Systems Based on High Performance Bulk and Film Thermoelectric Modules. *Journal of Thermoelectricity*, (1), 60–80. https://doi.org/10.63527/1607-8829-2025-1-60-80

Introduction

Growing demand for energy together with the need for non-polluting energy sources necessitates the search for novel types of electric converters, typically with direct energy conversion functionality [1 – 3]. The Sun is probably the most abundant and widespread source of energy on the Earth, which is available almost everywhere, albeit in different quantities. The Sun is the source of almost any energy type, be it wind energy, fossil fuels, hydropower, biomass energy or even nuclear energy (if we consider the emergence of heavy elements such as uranium as a result of supernova explosions). Solar energy reaches the Earth's surface at a rate of 120 petawatts [4]. This means that all the solar energy received in one day can meet the needs of the whole world for more than 20 years [4]. Although our needs increase from year to year by a few percent (Fig. 1), this renewable and inexhaustible energy source will be available during the entire period of existence of the Earth. Moreover, its power will grow in the long term due to the increase in the diameter of the Sun.

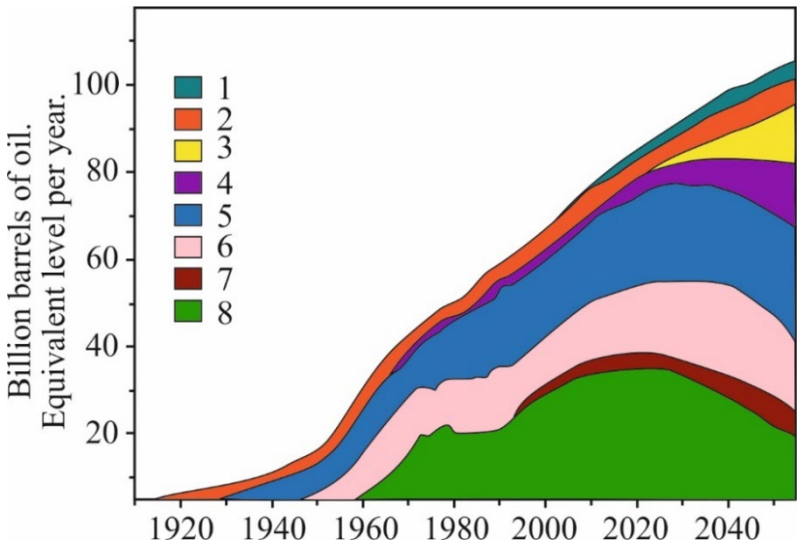

Fig. 1. World energy demand and forecast [4]. 1 – biofuels, 2 – hydroelectric, 3 – solar, wind, geothermal, 4 – nuclear electric, 5 – coal, 6 – natural gas, 7 – shale/tar sands, 8 – crude oil

There are many ways to utilize solar energy: electricity generation, photochemistry, solar desalination and room temperature control Among them, there is direct conversion of solar energy to electricity using photovoltaic cells and thermoelectric converters [5, 6]. The latter have an advantage, since they convert the energy of the entire solar spectrum through heating and creation of temperature gradient across the converter, while photovoltaic converters use only part of the spectrum (Fig. 2) limited by the band gap energy of semiconductor they are made of. Moreover, waste heat, the source of which is not only the Sun but also cooling radiators of various devices, as well as the surfaces of photoelectric converters that heat up during operation, can be also converted. Therefore, this way of collecting and converting solar energy into electricity will be widely applied having a profound impact on our society. Therefore, it has attracted the attention of researchers.

The efficiency of a thermoelectric generator (TEG) is the product of two terms, namely the Carnot and the thermoelectric efficiency. The corresponding equation is presented in [9].

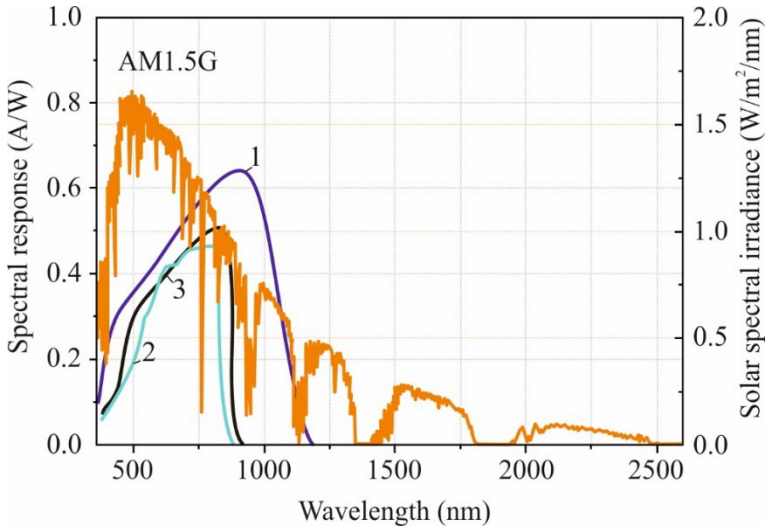

Fig. 2. Spectral dependences of solar power irradiance at AM1.5G conditions and response of the different efficient solar cells [7, 8]. 1 – Si, 2 – CdTe, 3 – GaAs

Since the first suggestion by A.F. Ioffe, semiconductors have been considered to be the best thermoelectric (TE) materials [9]. At electron (hole) concentrations $n(p) \sim 1 \times 10^{19}$ cm^{-3} heat transport through semiconductors is mainly determined by phonons. At such carrier concentrations, the Fermi level E_F is close to the bottom of conduction band E_C for *n*-type semiconductors or to the top of valence band E_V for *p*-type semiconductors.

Prof. Z. Dashevsky indicated three main parameters that determine the figure of merit *Z*. These are the effective mass of carriers (m_n* in *n*-type and m_p* in *p*-type semiconductors, respectively), the carrier mobility μ and the phonon thermal conductivity k_L. The equation for *Z* as the function of these parameters is presented in [9].

The values of *ZT* for different thermoelectric materials in the operating temperature range of 300 – 1200 K are published in [10 – 29]. Unfortunately, no thermoelectric material with optimal *ZT* over the wide temperature range is available now. The legs of typical commercial thermoelectric generators are conventionally fabricated from one type of semiconductor materials.

Therefore, a way to increase the efficiency of thermoelectric converters is the creation of multilayer (multistage) thermoelectric unicouples. Such approach can provide optimal average values of figure of merit *ZT* over a wide temperature range.

2. Technology

2.1. Hot pressing

The *n*- and *p*-type Bi_2Te_3 based compounds were prepared using a hot pressing technique, which is a high-pressure (100 ton) powder metallurgy process for forming powder compact at high temperature of ~ 670 K, sufficient to induce sintering (operating time ~ 0.5 h) (Figure 3). The process was carried out in argon atmosphere [9]. Before hot pressing, the materials were synthesized in evacuated silica tubes. After that, the compounds were crushed into powder. The advantage of hot pressing technique is preparation of highly textured Bi_2Te_3 based compounds

[9]. These compounds are characterized by remarkable anisotropy due to their crystal structure, which is the basis for anisotropy of thermoelectric conversion efficiency.

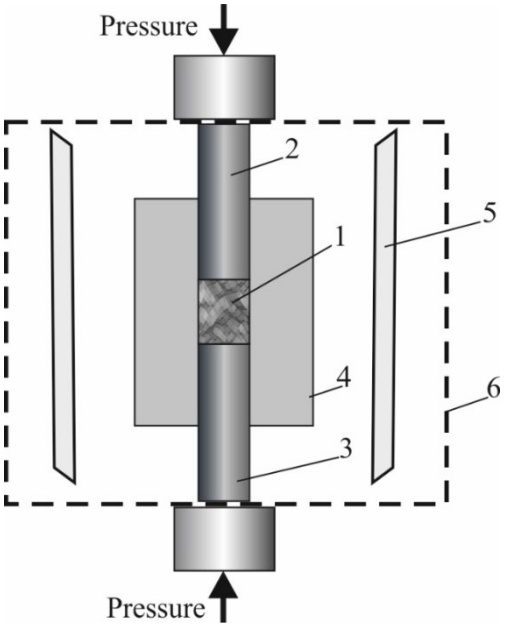

Fig. 3. Schematic view of hot pressing setup. 1 – material powder, 2 – top plunger, 3 – bottom plunger, 4 – die, 5 – heating elements, 6 – vacuum chamber

2.2. Spark Plasma Sintering (SPS) technique

The *n*-type $Pb_{1-x}In_xTe_{1-y}I_y$, *p*-type $Pb_{1-x}Tl_xTe$ and *p*-type $Ge_{1-x}Bi_xTe$ were prepared using Spark Plasma Sintering (SPS) technique [24 – 29]. The powder was compacted at 1 GPa in a protective atmosphere at room temperature to form tablets 20 mm in diameter and 5 mm thick. Then the tablets were heated at a rate of 50 K/min and sintered by SPS at 870 K for 20 min in argon atmosphere under axial compressive stress of 60 MPa. The schematic view of SPS unit was presented in [9].

2.3. Flash evaporation technique for preparation of thin thermoelectric films

The *p*-$Bi_{0.5}Sb_{1.5}Te_3$ and *n*-PbTe:In (I) films were deposited by flash evaporation technology, first proposed by Prof Z. Dashevsky in 1974. A setup for obtaining films by this method is shown in Fig. 4. $Bi_{0.5}Sb_{1.5}Te_3$ or PbTe:In(I) powder was introduced into the preheated quartz crucible (1) from a mechanically shaken powder vessel (7) [30, 31]. The evaporator was a quartz crucible (1) with a molybdenum wire heater (2) surrounded by a molybdenum heat screen (3). The powdered material was introduced into the crucible through a water-cooled channel (6). The substrate was heated by a substrate heater (5). All parts of the device were located in a chamber (8) under the vacuum of 10^{-5} mbar. The temperature of substrate during film preparation was T_s = 523 – 573 K; the evaporation velocity was v_e = 0.1 μm/min. After the evaporation process, all films were annealed in the same evaporation chamber at T_t = 623 K for 0.5 h in pure argon atmosphere at the pressure of p = 0.9 atm.

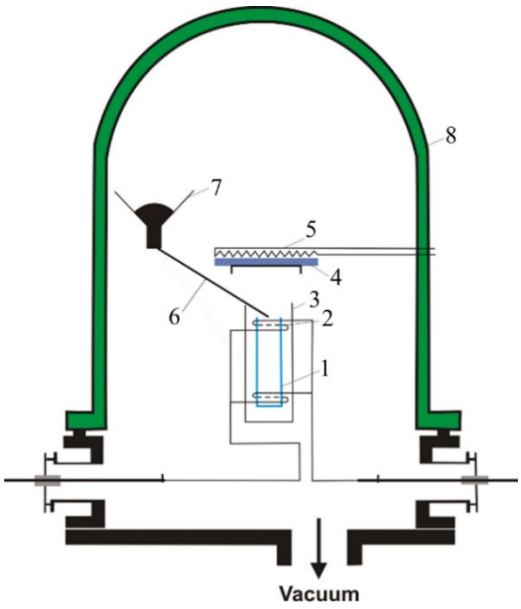

Fig. 4. Schematic view of the flash evaporation setup: 1 – quartz crucible, 2 – crucible heater, 3 – heat shield, 4 – substrate, 5 – substrate heater, 6 – channel, 7 – powder vessel, 8 – vacuum chamber

3. Characterization

3.1. Development of measurement setup for thermoelectric module characterization

Development and widespread use of thermoelectric generation as a user-friendly technology for direct energy conversion is mainly limited by small efficiency factors. Currently, the main efforts of scientists in the field of thermoelectricity are focused on increasing thermoelectric efficiency Z in wide range of operating temperatures (300 – 900 K). The main parameters that determine the quality of a thermoelectric material are the Seebeck coefficient, electrical conductivity and thermal conductivity. Moreover, electrical and operational characteristics, in particular internal resistance, generated current and voltage, thermoelectric power, heat capacity, etc are also crucial for the efficiency of thermoelectric power converters. All these parameters were measured by direct method [32]. A heat flow passed through a thermoelement due to the temperature gradient created between the heater and the cooler. A feature of the developed technique is the use of two identical samples placed on both sides of the heater and cooled by identical water radiators. The measuring cell is schematically shown in Fig. 5.

Cooling with running water made it possible to maintain stable temperature of cold junctions. To heat cylindrical or rectangular samples, a miniature low-power copper heater was made, which in combination with a tubular tantalum heat shield made it possible to significantly reduce parasitic heat losses, difficult to take into account.

To diagnose ready-made thermoelectric energy conversion modules with the size of 40×40 mm^2, a rectangular copper heater with the size of $40 \times 40 \times 8$ mm^3 was made. It contacted the hot surfaces of the thermocouple through the thermal interface. The general view of the measuring cell is shown in Fig. 5 b.

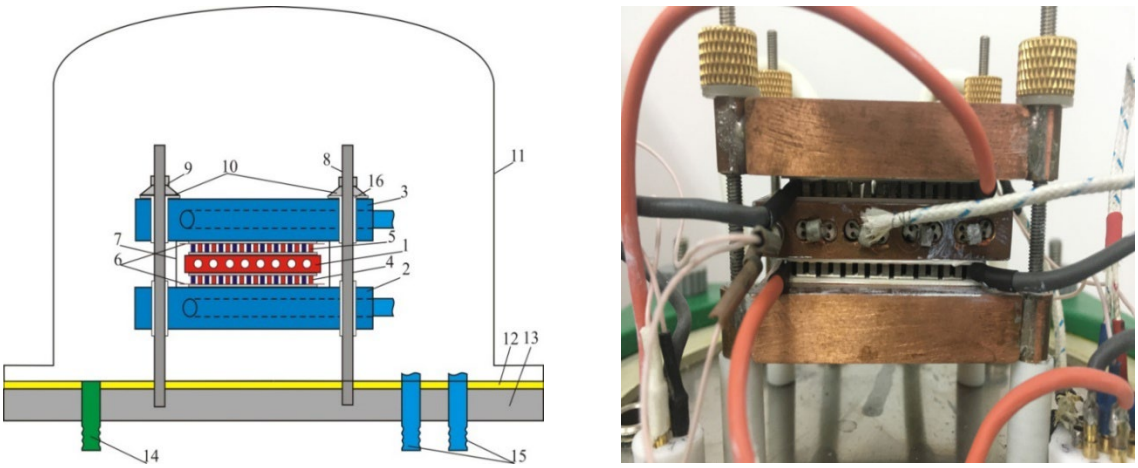

a) *b)*

Fig. 5. Schematic view of the measuring cell (a) and the photo of the measuring cell with installed thermoelectric elements (b). 1 – copper electric heater with thermocouple and 2, 3 – copper water radiator with thermocouple, 4, 5 – thermocouples or single samples of thermoelectric material, 6 – electrical contacts, 7 – heat shield, 8 – clamping pins, 9 – nuts, 10 – spring washers, 11 – vacuum cap, 12 – vacuum gasket, 13 – base, 14 – fitting for pumping, 15 – fittings for water supply and drainage, 16 – fluoroplastic insulation

The design also provides the possibility of installing an additional heater on two additional threaded racks. This heater is installed at the level of the interface of the two radiators. This allows the study of film thermocouples, with the cold side clamped between two radiators, and the hot side is pressed by a copper plate to the additional heater.

All electrical contacts are routed through two sealed connectors located in the base. The setup supports up to 5 thermocouples. One thermocouple can be located in the heater, another one in the radiators, and two others can be drilled in the sample for additional control of heat fluxes. When the electrical properties of semiconductors are studied, such basic parameters as electrical conductivity, Seebeck coefficient and thermoelectric power are measured.

The efficiency of TE unicouple (TE module) is defined as:

$$\eta = (P_1 + P_2)/Q, \quad (1)$$

where P_1 and P_2 are the electric power of the upper and the lower thermoelectric unicouple (or thermoelectric module), and Q is the heater power, respectively.

The temperature of the heater is changed in the range of 400 – 900 K with an accuracy of 2 %. The temperature of the radiators is controlled by a thermostat at ~ 300 K with the accuracy of 1 %. The estimated accuracy of efficiency measurement is ~ 3 %.

4. High-performance thermoelectric materials for application in energy systems

4.1. Low-temperature (300 – 600 K) thermoelectric materials based on *n*-type and *p*-type Bi_2Te_3-based compounds

Bismuth telluride based compounds, namely *n*-type $Bi_2Te_{3-x}Se_x$ and *p*-type $Bi_{2-x}Sb_xTe_3$ solid solutions are the most effective thermoelectric materials operating at temperatures up to

$T_h \sim 600$ K [12 – 19].

Temperature dependences of the Seebeck coefficient S, electrical conductivity σ, thermal conductivity κ and dimensionless figure of merit ZT in the temperature range of 300 – 600 K for p-type $Bi_{0.5}Sb_{1.5}Te_3$ prepared by hot pressing or SPS technique were presented in [9, 13].

The Seebeck coefficient S achieves maximum for all specimens and then decreases with a rise in temperature. As shown in [9], such behavior of S is related to appearance of electrons, which induce a negative value of S coefficient. In this case, S is determined as follows [9]:

$$S = \frac{(S_p\sigma_p + S_n\sigma_n)}{\sigma_n + \sigma_p}, \quad (2)$$

where indices n and p describe parameters for electrons and holes, respectively.

The electron mobility is higher than the hole one [9]. The electron concentration increases exponentially with temperature. In this case, we observe the sharp decrease of S. According to Eq. 2, the Seebeck coefficient becomes anisotropic at high temperatures due to presence of opposite-sign charge carriers. As shown in [9], the negative effect of minority charge carriers is minimized in crystals with the orientation parallel to the axis C. At $T > 500$ K, it results in higher values of the dimensionless figure of merit ZT for samples with the orientation parallel to this axis [9].

Temperature dependence of the Seebeck coefficient S, electrical conductivity σ, thermal conductivity κ and dimensionless figure of merit ZT in the temperature range of 300 – 600 K for n-type $Bi_2Te_{3-x}Se_x$ samples prepared by hot pressing were presented in [9, 13, 18]. Such temperature behavior of S, σ, and κ defines the maximum value of $ZT \sim 1.2$ for the optimal composition of $Bi_2Te_{2.7}Se_{0.3}$ solid solution with electron concentration $n \sim 5 \times 10^{19}$ cm^{-3} and $S \approx -165$ μV/K at $T \sim 300$ K. Consequently, the best TE material for n-type legs in thermoelectric low temperature converters is hot-pressed SbI_3-doped n-$Bi_2Te_{2.7}Se_{0.3}$ alloy.

4.2. Medium-temperature (600 – 900 K) n-type thermoelectric materials based on PbTe semiconductor compound

The maximal value of the figure of merit Z as a function of electron density depends on the location of the Fermi level E_F relative to the bottom of the conduction band E_C. It was shown that indium dopant in PbTe makes optimal the location of the Fermi level by creation of indium quasi local level in the conduction band. This leads to so-called pinning of the Fermi level [33, 34]. The indium level is the source of electrons which mitigate the influence of minority carriers (holes). This effect makes the average figure of merit $(ZT)_{av}$ significantly higher over a wide temperature range. Additional improvement of $(ZT)_{av}$ was achieved by co-doping PbTe with iodine, which is a well-known donor impurity for this material [35].

Temperature dependences of the Seebeck coefficient, electrical conductivity, thermal conductivity and the dimensionless figure of merit ZT in the temperature range of 600 – 900 K for n-type $Pb_{1-x}In_xTe_{1-y}I_y$ specimens prepared by SPS were presented in [25]. The maximum value of ZT for $Pb_{0.999}In_{0.001}Te_{0.999}I_{0.001}$ was close to 1.3 at $T = 750$ K, which is one of the highest values of ZT for n-type PbTe.

4.3. Medium-temperature (600 – 900 K) *p*-type thermoelectric materials based on GeTe compound

The *p*-type thermoelectric was based on GeTe semiconductor compound doped by Bi up to 5 atomic %. This enabled to decrease significantly the hole concentration to the optimal value from the point of view of TE efficiency (*ZT*) [27]. On the other hand, this TE material has satisfactory mechanical characteristics, in contrast with high-efficiency *p*-type PbTe. This property is very important for application in thermoelectric energy modules [9].

Temperature dependences of the Seebeck coefficient, electrical conductivity, thermal conductivity and the dimensionless figure of merit *ZT* for *p*-type $Ge_{1-x}Bi_xTe$ prepared by SPS in the temperature range of 600 – 900 K were presented in [28].

The $Ge_{0.96}Bi_{0.04}Te$ specimen has the lowest value of $\kappa \approx 2$ W/m K at 600 K, which is more than twice less than that for GeTe specimen. This trend is observed up to T = 900 K. The dimensionless figure of merit *ZT* for $Ge_{0.96}Bi_{0.04}Te$ specimen reaches the value of ~ 2.0 at T = 700 K and remains virtually constant up to 900 K. This value is more than twice the value of *ZT* for pure GeTe. The average thermoelectric figure of merit for $Ge_{0.96}Bi_{0.04}Te$ specimen $(ZT)_{av} \sim 1.3$ has been obtained for the operating temperature difference ΔT = 300 K (T_c = 900 K, T_h = 600 K). For comparison, the thermoelectric properties of a high-performance *p*-type $Pb_{0.94}Tl_{0.02}Na_{0.002}Te$ prepared by SPS [26] demonstrate higher value of *ZT* for the $Ge_{0.96}Bi_{0.04}Te$ specimen.

5. Applications

5.1. Thermoelectric module

To obtain maximum TE efficiency, we propose to fabricate composite TE modules (TEMs) from multilayer unicouples designed for given temperature gradients, following the suggestion of Prof. Z. Dashevsky [9]. Each stage should be made of a different material layer. Each material was selected such that its *ZT* is maximal in the temperature range prevailing in the corresponding stage.

The structure and the composition of a multilayer (multistage) TE unicouple designed for operation in the temperature range of 300 – 900 K are presented in Fig. 6. The first layer material was prepared from low-temperature TE materials (the temperature interval is 300 – 600 K) based on *n*-type and *p*-type Bi_2Te_3 fabricated by hot pressing (layers 2 and 5). The second and the third layer materials for *n*- type thermoelectric leg were PbTe based compounds, namely PbTe doped by iodine (3) and $Pb_{0.999}InTe_{0.999}I_{0.001}$ (4). The second layer of *p*-type thermoelectric leg was prepared from $Ge_{1-x}Bi_xTe$ (7) by Spark Plasma Sintering (SPS). The metallic contacts were fabricated by hot pressing, namely the cobalt layer (1) as the contact between *n*-type and *p*-type legs on the cold side and the iron layer (9) as the contact between *n*-type and *p*-type legs on the hot side. A thin layer of heavy doped *p*-type SnTe (8) prepared by SPS was used for decreasing contact resistance for *p*-leg on the hot side.

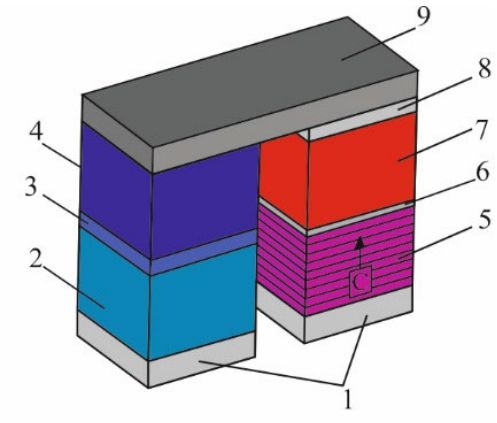

Fig. 6. Schematic view of a multilayer thermoelectric generator unicouple for the temperature range T_c = 320 K and T_h = 900 K. 1 – metallic contact from Co + 6 wt % Bi prepared by hot pressing. 2 – n-type TE layer prepared by hot pressing of n-$Bi_{2.7}Se_{0.3}Te_3$. 3 – n-type TE layer made by SPS of n-$Pb_1Te_{0.999}I_{0.001}$. 4 – n-type TE layer prepared by SPS of n-$Pb_{0.999}In_{0.001}Te_{0.999}I_{0.001}$. 5 – p-type TE layer prepared by hot pressing of p-$Bi_{0.5}Sb_{1.5}Te_3$, oriented along the axis C. 6 – thin anti-diffusion layer prepared by hot pressing of $CoGe_2$ compound. 7 – p-type TE layer prepared by SPS of p-$Ge_{0.96}Bi_{0.04}Te$. 8 – thin heavily doped p-type SnTe layer prepared by SPS for improving ohmic contact. 9 – Fe metal contact on the hot side prepared by hot pressing

Several multi-layer unicouples were fabricated, and their efficiency was measured using the setup described in subsection 3.1. The experiments showed that the energy conversion efficiency reached a high value of ~ 14 – 15 % when operated between the hot temperature T_h = 900 K and at cold temperature T_c = 320 K.

Fabrication of the proposed thermoelectric module (TEM) (Fig. 7) may include the following steps:

1. Assembly of the developed TE unicouples into an aluminum cassette (Fig. 7 *a*).
2. Sintering the cassette by hot pressing (during 0.5 h at T_h = 700 K in argon atmosphere) (Fig. 7 *b*).
3. Formation of a chain of thermoelements connected in series.
4. Assembly of the TE module in a protective case of stainless steel thin sheet (argon atmosphere).

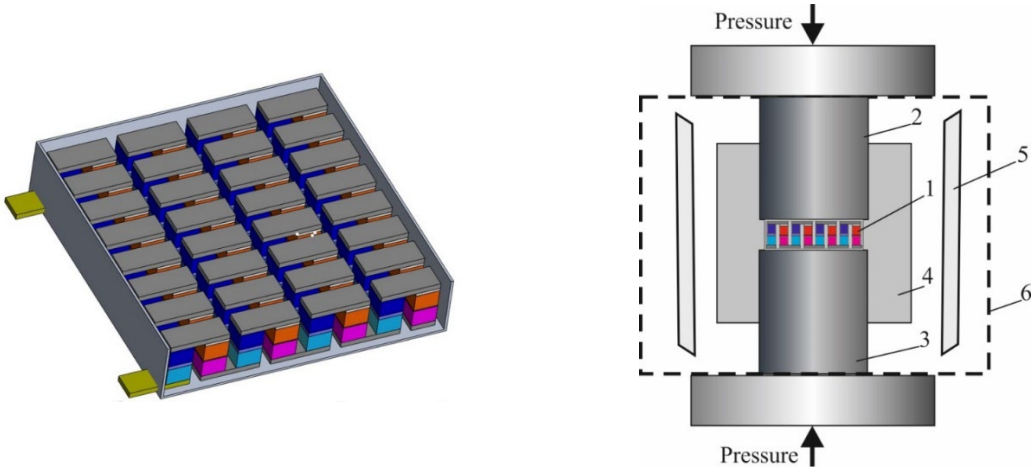

a) *b)*

Fig. 7. Assembly of the thermoelectric unicouples into an aluminum cassette (a). Sintering process (b)

Table 1

Characteristics of thermoelectric module.

Dimensions, mm-mm-mm	Quantity of unicouples	Hot temperature, T_h, K	Cold temperature, T_c, K	Outside voltage U, V	Current I, A	Electric power P_e, W
100-20-10	50	900	300 – 320	4	20	80

5.2. Solar Thermoelectric System (STES)

The first design of gas thermoelectric generator with electric power of 170 W and efficiency ~ 8 % based on multistage thermoelectric modules (T_h = 800 K, T_c = 350 K) was developed in the laboratory of Prof. Z. Dashevsky in 1993. These TEGs provided a high reliability and long operative time of ~ 25 years [9].

The schematic view of a novel Solar Thermoelectric System (STES) is shown in Fig. 8. Solar radiation is collected by the light receiver (1) with the tracking system (2) (heliostat) and directed to the absorber (3). Heat is accumulated in the thermal storage part (4) of STES in the phase change material, the melting temperature of which is close to the optimal operating temperature of the thermoelectric module (TEM) (6). Part of the thermal energy (up to 15 %) is converted into electrical energy due to the difference ΔT between the temperatures of the solar absorber (3) and radiators (7) on the cold side of the TEM. The cold part of the TEM is in contact with the radiator (7) equipped with the heat pipes (8) [36] to intensify the heat flow and direct it to the external radiators (9). In a conventional TEM, cooling radiators dissipate most of the thermal energy into the environment [37] due to convection and irradiation. Here, it is proposed to use a special type of photonic radiative cooler [38 – 41] with enhanced radiative part.

5.2.1. Light collector

The solar collector is a Fresnel lens [37] with a Sun tracking system - a heliostat [38]. Its main features are that it is a thin plastic sheet embossed with concentric grooves having triangular profile. The area of such lens is calculated from the operating power of TEMs and for 5 kW it should be about 5 ÷ 6 m^2. Such collector has simple design, high accuracy, low weight and cost. The low weight combined with the heliostat, also ensures high tracking accuracy when small motors and drive mechanisms are used.

Sun tracking applies polar coordinate system (the same basic mechanism as in a watch) for easy and accurate tracking. In addition, the unique design, combining the main axes of movement with the optical axis, allows directing concentrated solar radiation to a stationary receiver with a small round window.

A design of the type of hollow integrating sphere made of a low emissivity material (e.g., stainless steel or molybdenum) is proposed for the receiver of solar radiation. The surface of the sphere can be optionally covered with a heat-resistant light-absorbing material such as carbon black or carbon nanotubes [39]. Such surface itself absorbs well solar radiation due to microroughness. Moreover, reflected and scattered energy falls on other parts of the sphere, where it is additionally absorbed. The energy loss in such receiver is caused by only a small

part of the radiation reflected and back out through the small receiving window of the sphere, which can be additionally covered by quartz window with antireflection coating [40]. Such window transmits solar light and reflects back low energy photons coming out from the heated sphere thus reducing solar energy loss.

5.2.2. Thermal energy storage

The thermal storage (Fig. 8) is based on a phase change material (PCM) with the latent heat of fusion used for energy storage. A solar receiver (3) is integrated into the storage vessel (4). This is done in order to ensure even absorption and to reduce thermal and hydrostatic loads (i.e. formation of local liquid pockets where high pressure may develop). The energy absorbed by such sphere makes PCM in the accumulator of the system heat and melt. Such battery uses the accumulated energy of phase transition to maintain the temperature of the hot end of the thermal converter to generate electricity during the dark part of the day. Current design proposes to use Al with melting point around 923 K as PCM. Al is non-toxic, environmentally harmless and readily available. Moreover, it has relatively high heat of fusion, ensuring high storage density (400 Joules per gram). Finally, the melting temperature of Al can be tuned to 900 K by alloying with Cu, which is appropriate for the intended optimal high-end temperature of the system.

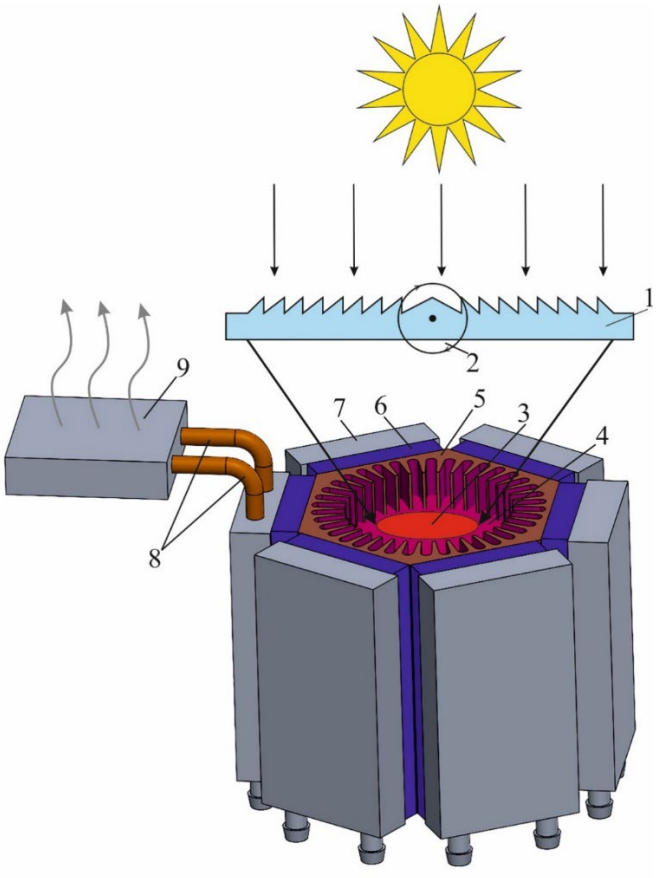

Fig. 8. Schematic view of Solar Thermoelectric System (STES): 1 – Fresnel lens, 2 – heliostat, 3 – solar receiver input (black body), 4 – thermal storage (Al alloy), 5 – heat exchanger, 6 – thermoelectric module (TEM), 7 – heat sink with heat pipes, 8 – heat pipes, 9 – photonic radiative cooler

To roughly estimate the weight of Al needed to save thermal energy in the form of the energy of melting for the system with heat power Q = 5 kW, we have to divide the collected energy during 12 hours of day time by the Al specific heat of fusion h = 10.79 kJ/mol and multiply by the Al molar mass M = 26.98 g/mol. The resulting weight of Al is about 540 kg.

5.2.3. Thermoelectric power unit (TPU)

A schematic view of a TPU is presented in Fig. 8. When it is considered to apply within an autonomous solar energy converter, it can be classified from the point of view of capacity, energy quality, operating temperature, location and utilization of heat. The temperature of heat exchanger (5) connected with TPU is stable at about 900 K. Conceptual design of TPU was produced for heat exchanger (5) by square $F = 1\ m^2$ and heat power Q = 5 kW. TPU consists of 6 TEMs (6) connected electrically in series and thermally in parallel. The cold side of each TEM is connected to the heat sink (7) equipped with heat pipes (8) [36]. The coolant in heat pipes is acetone solution at the temperature of 310 K.

Heat pipes intensify heat flow and direct it to external radiators (9) of photonic radiative cooler of a special type [41] with enhanced radiative part. The enhanced radiative cooling at the ambient air temperature under direct sunlight was experimentally demonstrated. Such thermal emitter reflects 97 % of incident sunlight while emitting strongly and selectively in the atmospheric transparency window of 8÷13 μm. Under direct sunlight with the power exceeding 850 watts per square meter, the photonic radiative cooler cools to around 5 K below ambient air temperature and has a cooling power of 40.1 watts per square meter at ambient air temperature.

We expect that the prototype of such a hybrid system can produce ~ 400 – 500 W of electrical energy. The rest of thermal energy can be potentially used for domestic heating and hot water supply. The advantage of such system is high stability without operative service during about one year and long life time not less than ~ 20 – 25 years.

6. Development of high-performance film thermoelectric module for solar applications

Presently, micro-energy converters for energy harvesting are more useful than standard electrical batteries. They have become realizable due to drastic decrease in power consumption of electronic components caused by advances in the field of electric energy storage, miniaturization, and optimization [42 – 50]. These films were fabricated by co-evaporation, molecular beam epitaxy, hot wall technique, magnetron sputtering and pulsed laser deposition. However, high value of the figure of merit Z for Bi_2Te_3-based films comparable to that for bulk crystals ($Z \sim 3 \times 10^{-3}\ K^{-1}$) [9] was not achievable for a long time. Recently, the high value of $Z \approx 3 \times 10^{-3}\ K^{-1}$ at T = 300 K for p-type $Bi_{0.5}Sb_{1.5}Te_3$ films was obtained in the laboratory of Prof. Z. Dashevsky [30].

For film preparation, thin polyimide substrate with the thickness of ~ 10 μm was used to minimize negative heat wastes. The benefits of polyimide material are the extremely low thermal conductivity (~ 3.5 $Wcm^{-1}K^{-1}$) and high flexibility [51]. Use of a flexible polyimide

substrate and perforation cuts between *p*-and *n*-legs allowed us to develop a compact (packaged) design of Film Thermoelectric Module (FTEM).

6.1 Thermoelectric properties

All *p*-type ($Bi_{0.5}Sb_{1.5}Te$ + 0.5 wt. % Te and $Bi_{0.5}Sb_{1.5}Te$ + 1.0 wt. % Te) and *n*-type ($Pb_{0.9995}In_{0.0005}Te$ and $PbTe_{0.9996}I_{0.0004}$) films were prepared on a thin flexible polyimide substrate [51].

Fig. 9 *a* presents the Seebeck coefficient *S* for these films over the entire temperature range of 300 – 600 K. The temperature trend of the Seebeck coefficient for *p*-type films shows the maximum and then goes down due to the effect of intrinsic carriers, which is typical for narrow-band gap semiconductors.

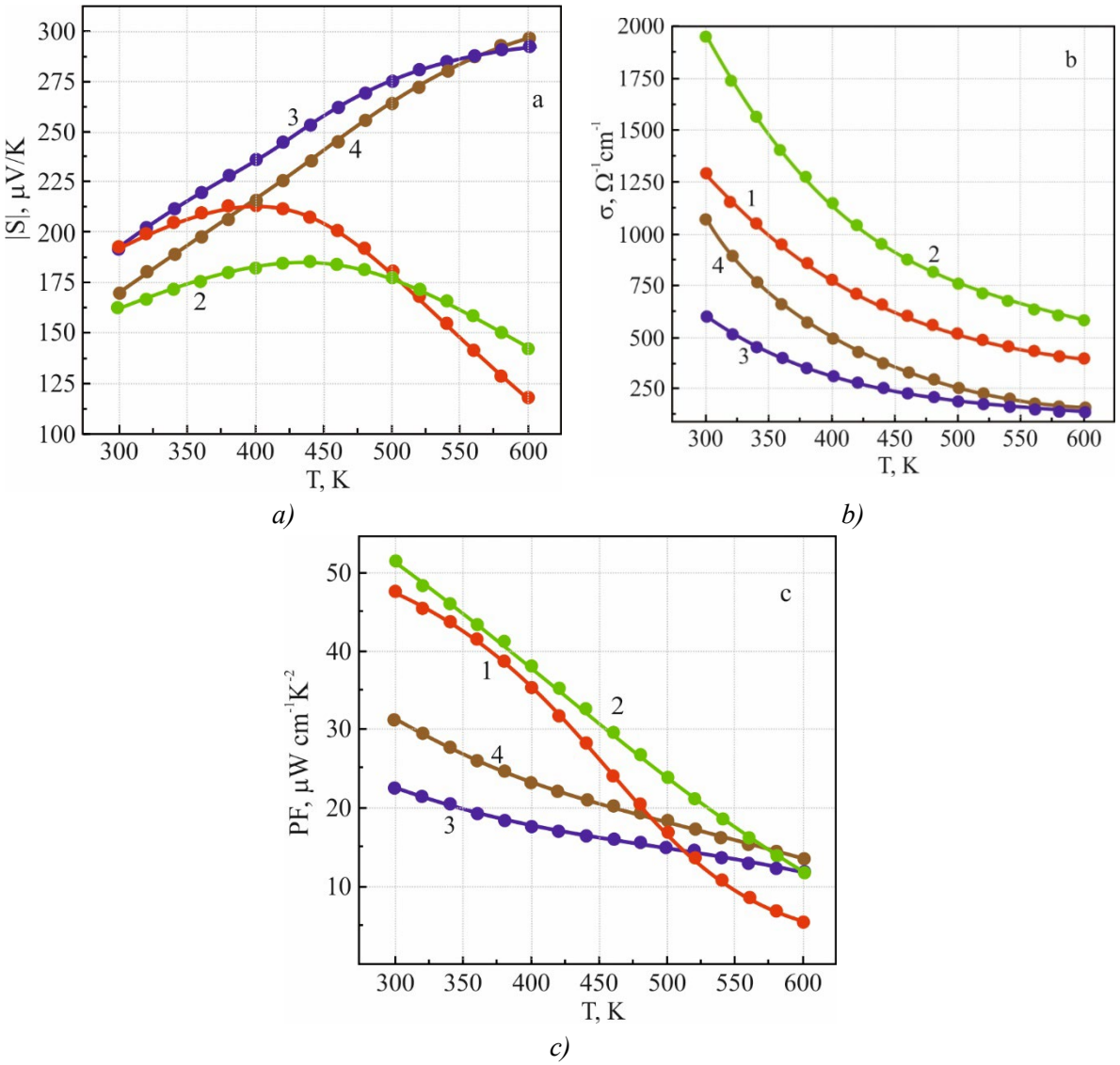

a) *b)* *c)*

Fig. 9. Temperature dependence of the Seebeck coefficient S (absolute value) (a), electrical conductivity σ (b) and Power factor $P = S^2\sigma$ (c) as a function of temperature for p-and n-type thermoelectric films prepared by flash evaporation. 1 – p-type $Bi_{0.5}Sb_{1.5}Te$ + 1.0 wt. % Te. 2 – p-type $Bi_{0.5}Sb_{1.5}Te$ + 0.5 wt. % Te. 3 – n-type $Pb_{0.99}In_{0.01}Te$. 4 – $PbTe_{0.99}I_{0.001}$

Electrical conductivity of the investigated films decreases over the investigated temperature range indicating a metallic character (Fig. 9 *b*). Excellent thermoelectric performance of the fabricated films was confirmed by estimation of the Power Factor $P = S^2\sigma$. (Fig. 9 *c*). The maximum value was $S^2\sigma \approx 50$ W/cmK at $T = 300$ K for *p*-type films, which is practically equal to the power factor for the best bulk samples with the same chemical composition [13, 25].

Table 2 presents measured thermoelectric characteristics (the Seebeck coefficient *S*, electrical conductivity σ and thermal conductivity κ) at $T = 300$ K for *p*-type and *n*-type films of different compositions. The measurement method for *S,* σ and κ are presented in [31].

Table 2

Thermoelectric properties of p-type $Bi_{0.5}Sb_{1.5}Te_3$ and n-type PbTe:In films and bulk crystals at T = 300 K

Composition	Type of material	Seebeck coefficient *S*, μV/K	Electrical conductivity σ, $\Omega^{-1}cm^{-1}$	Thermal conductivity $\kappa\times10^3$, W/cm.K	Figure of merit $Z\times10^3$, K^{-1}	Ref.
$Bi_{0.5}Sb_{1.5}Te_3$ + 1.0 wt. % Te	film	190	1250	15	3.0	
$Pb_{0.999}In_{0.001}Te$	film	– 190	670	20	1.2	
$Bi_{0.5}Sb_{1.5}Te_3$	bulk	200	1150	16	3.0	[13]
$Pb_{0.999}In_{0.001}Te$	bulk	– 200	600	23	1.1	[24]

6.2. Solar film thermoelectric module (FTEM) on flexible substrate

Fabrication of FTEM includes the following stages:

1. Preparation of *p*-type $Bi_{0.5}Sb_{1.5}Te_3$ film legs with the thickness of ~ 3 μm on both sides of the polyimide substrate (~ 10 μm).
2. Preparation of *n*-type $Pb_{0.99}In_{0.01}Te$ film legs with the thickness of ~ 3 μm on both sides of the polyimide substrate.
3. Fabrication of perforations between *p*- and *n*-type legs. The size of the cut is ~ 0.2 mm and the distance between the cuts is ~ 1 mm.
4. Fabrication of electrical connection between the *p*- and *n*-type legs by Cr and Au layers with the thicknesses of 0.1 and 1 μm, respectively, on both sides of the polyimide substrate and inside the perforation cuts.
5. Fabrication of a thin protective coating with the thickness of ~ 0.5 μm on both sides of the FTEM by plasma-chemical method of cyclohexane polymerization [52].

Schematic view of the main stages of fabrication of the flexible FTEM based on *p*-

$Bi_{0.5}Sb_{1.5}Te_3$ and *n*-PbTe:In thermoelectric materials is presented in Fig. 10.

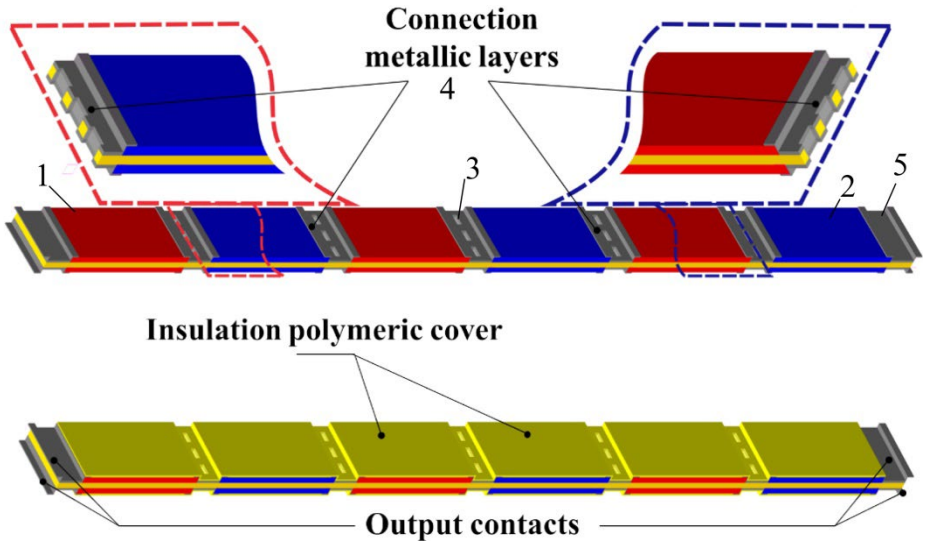

Fig. 10. Schematic view of FTEM.: a) – planar design. b) a view of the film module after protective coating. 1 – p-legs. 2 – n-legs. 3 – perforation, 4 – metallic connecting layers between legs, 5 – output electric contacts

6.3. Solar application of FTEM

FTEM can be used for fabrication of film solar thermoelectric converter (generator). The principle of its operation may be described as follows: the incoming solar radiation creates a temperature gradient across FTEM, which generates electricity due to the thermoelectric effect. A schematic view of the proposed solar thermoelectric converter is presented in Fig. 11. The electric voltage was induced by heating the hot side of the film thermoelectric unicouples. The cold side temperature of the film thermoelectric unicouples was stabilized by a black body with the temperature of 300 K.

The flexible polyimide substrate and perforation cuts between *p*-and *n*-legs allow to bend substrate along the perforation and to create a compact (packaged) design of the FTEM.

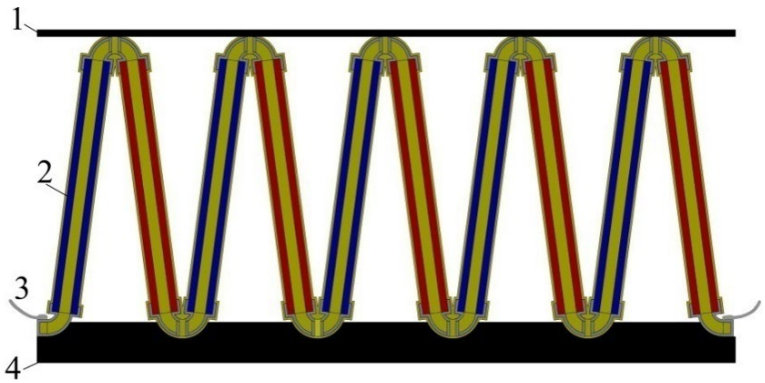

Fig. 11. Schematic view of Solar Film Thermoelectric Converter (SFTEC). 1 – absorption layer. 2 – FTEM on flexible (polyimide) substrate. 3 – electric contacts. 4 – heat sink (black body)

Such film thermoelectric converters with output voltage of several volts and electric power of several microwatts at the temperature of the hot side of FTEM $T_h \sim 400$ K can be used in solar energy micro-systems.

Conclusions

Due to the increase in energy demand and depletion of natural resources, the development of energy harvesting technologies becomes very important. High reliability and long operation time lead to a wide use of TEGs in space industry and gas pipe systems. Further development and wider application of solar TEGs is mainly limited by their relatively low conversion efficiencies. To overcome this issue, we suggest for the first time to use direct conversion of solar energy by a high-perfection thermoelectric modules for creation of autonomic systems with electric power up to 500 W and electric efficiency up to 15 %.

To achieve this goal, unique multilayer (multistage) thermoelectric module was developed. Two types of high-efficiency thermoelectric materials were selected to ensure a wide range of operating temperatures.

The first type is the "low-temperature" thermoelectrics (300 – 600 K temperature range) based on Bi_2Te_3 compounds (*n*-type solid solutions $Bi_2Te_{3-x}Se_x$, *p*-type solid solution $Bi_{0.5}Sb_{1.5}Te_3$ with orientation along the crystal axis C), obtained by hot pressing in argon atmosphere.

The second type is the "medium-temperature" thermoelectrics (600 – 900 K temperature range) prepared by modern SPS technique. For the *n*-type thermoelectrics were used two stages – the first stage – classic PbTe doped by iodine and second stage – novel material PbTe doped by indium, creating the resonance level at the conduction band, which provided practically constant value of average figure of merit *ZT* at wide temperature range. Thermoelectrics of *p*-type were based on GeTe semiconductor compound doped by Bi up to 5 atomic %. It allowed to decrease the hole concentration to the values close to the optimal one from the point of view of TE efficiency (*ZT*). On the other hand, this thermoelectric had satisfactory mechanical properties, in contrast with high-efficiency *p*-type PbTe.

We developed for the first time film thermoelectric modules on thin flexible substrate with the values of figure of merit *Z* comparable to those of bulk modules. Such film thermoelectric converters with output voltage of several volts and electric power of several microwatts can be used in solar energy micro-systems.

Author Contributions: S. Mamykin – Principal Investigator; B. Dzundza – Investigation and visualization; R. Shneck – Project Management and conceptualization; L. Vikhor – Calculations; Z. Dashevsky – Supervision.

Funding: This research received no external funding.

Conflicts of Interest: The authors declare that they have no known competing financial interests or personal relationships that could influence the work reported in this paper.

Authors' information

S. Mamykin – Ph.D. (Physics).
B. Dzundza – D.Sc. (Technical Sciences), Professor.
R. Shneck – D.Sc., Professor.
L. Vikhor – D.Sc. (Phys.-Math.).
Z. Dashevsky – D.Sc. (Phys.-Math.), Professor.

References

1. M.A. Zoui, S. Bentouba, J.G. Stocholm, M. Bourouis (2020). A review on thermoelectric generators: Progress and applications, *Energies*, 13, 3606.
2. D. Champier, Thermoelectric generators: A review of applications (2017). *Energy Conversion and Management* 140, 167 – 181.
3. L.N. Vikhor, L.I. Anatychuk (2009). Generator modules of segmented thermoelements, *Energy Conversion and Management* 50, 2366 – 2372
4. T.M. Maslamani, A.I. Omer, M. Majid (2014). Development of solar thermoelectric generator, E*uropean Scientific Journal* 10.
5. Z. Dashevsky, D. Kaftori, D. Rabinovich (1998). High efficiency thermoelectric unit within an autonomous solar energy converter, in: Seventeenth International Conference on Thermoelectrics. Proceedings ICT98 (Cat. No. 98TH8365), IEEE, 531 – 534.
6. S.S. Indira, C.A. Vaithilingam, K.-K. Chong, R. Saidur, M. Faizal, S. Abubakar, S. Paiman (2020). A review on various configurations of hybrid concentrator photovoltaic and thermoelectric generator system, *Solar Energy* 201, 122 – 148.
7. H. Field (1997). Solar cell spectral response measurement errors related to spectral band width and chopped light waveform, in: Conference Record of the Twenty Sixth IEEE Photovoltaic Specialists Conference-1997, IEEE, 471 – 474.
8. G. Huang, S.R. Curt, K. Wang, C.N. Markides (2020). Challenges and opportunities for nanomaterials in spectral splitting for high-performance hybrid solar photovoltaic-thermal applications: a review, *Nano Materials Science* 2, 183 – 203.
9. Dashevsky, A. Jarashneli, Y. Unigovski, B. Dzunzda, F. Gao, R.Z. Shneck (2022). Development of a High Perfomance Gas Thermoelectric Generator (TEG) with Possible Use of Waste Heat, *Energies* 15, 3960.
10. S. El Oualid, F. Kosior, A. Dauscher, C. Candolfi, G. Span, E. Mehmedovic, J. Paris, B. Lenoir (2020). Innovative design of bismuth-telluride-based thermoelectric micro-generators with high output power, *Energy & Environmental Science* 13, 3579 – 3591.
11. M.K. Rad, A. Rezania, M. Omid, A. Rajabipour, L. Rosendahl (2019). Study on material properties effect for maximization of thermoelectric power generation, *Renewable energy* 138, 236 – 242.
12. H. Mamur, M. Bhuiyan, F. Korkmaz, M. Nil, A review on bismuth telluride (Bi_2Te_3) nanostructure for thermoelectric applications (2018). *Renewable and Sustainable Energy Reviews* 82, 4159 – 4169.

13. M. Maksymuk, B. Dzundza, O. Matkivsky, I. Horichok, R. Shneck, Z. Dashevsky (2022). Development of the high performance thermoelectric unicouple based on Bi_2Te_3 compounds, *Journal of Power Sources* 530, 231 – 301.
14. C. Gayner, K.K. Kar (2016). Recent advances in thermoelectric materials, *Progress in Materials Science* 83, 330 – 382.
15. J.R. Sootsman, D.Y. Chung, M.G. Kanatzidis (2009). New and old concepts in thermoelectric materials, *Angewandte Chemie International Edition* 48, 8616 – 8639.
16. O. Ben-Yehuda, R. Shuker, Y. Gelbstein, Z. Dashevsky, M.P. Dariel (2007). High textured Bi_2Te_3-based materials for thermoelectric energy conversion. *Journal of Applied Physics* 101, 25 – 32.
17. D.-B. Hyun, J.-S. Hwang, J.-D. Shim, T.S. Oh (2001). Thermoelectric properties of $(Bi_{0.25}Sb_{0.75})_2Te_3$ alloys fabricated by hot-pressing method, *Journal of materials science* 36, 1285 – 1291.
18. Taras Parashchuk, Rafal Knura, Oleksandr Cherniushok, and Krzysztof T. Wojciechowski (2022). Ultralow Lattice Thermal Conductivity and Improved Thermoelectric Performance in Cl-Doped $Bi_2Te_{3-x}Se_x$ Alloys, *ACS Appl. Mater. Interfaces* 14, 33567 − 33579
19. R. Knura, M. Maksymuk, T. Parashchuk and K.T. Wojciechowski (2024). Achieving high thermoelectric conversion efficiency in Bi_2Te_3-based stepwise legs through bandgap tuning and chemical potential engineering, *Dalton Trans*. 53, 123
20. Y. Gelbstein, Z. Dashevsky, M. Dariel (2005). High performance *n*-type PbTe-based materials for thermoelectric applications, *Physica B: Condensed Matter* 363, 196 – 205.
21. T. Parashchuk, I. Horichok, A. Kosonowski, O. Cherniushok, P. Wyzga, G. Cempura, A. Kruk, K.T. Wojciechowski (2021). Insight into the transport properties and enhanced thermoelectric performance of *n*-type $Pb_{1-x}Sb_xTe$, *Journal of Alloys and Compounds* 860, 158355.
22. R. Knura, T. Parashchuk, A. Yoshiasa, K.T. Wojciechowski (2021). Origins of low lattice thermal conductivity of $Pb_{1-x}Sn_xTe$ alloys for thermoelectric applications, *Dalton Transactions,* 50, 4323 – 4334.
23. I. Petsagkourakis, K. Tybrandt, X. Crispin, I. Ohkubo, N. Satoh, T. Mori (2018). Thermoelectric materials and applications for energy harvesting power generation, *Science and technology of advanced materials* 19, 836 – 862.
24. T. Parashchuk, Z. Dashevsky, K. Wojciechowski (2019). Feasibility of a high stable PbTe: In semiconductor for thermoelectric energy applications, *Journal of Applied Physics* 125, 245103.
25. K.T. Wojciechowski, T. Parashchuk, B. Wiendlocha, O. Cherniushok, Z. Dashevsky (2020) Highly efficient *n*-type PbTe developed by advanced electronic structure engineering, *Journal of Materials Chemistry C* 8, 13270 – 13285.
26. T. Parashchuk, B. Wiendlocha, O. Cherniushok, R. Knura, K.T. Wojciechowski (2021). High thermoelectric performance of *p*-type PbTe enabled by the synergy of resonance scattering and lattice softening, *ACS Applied Materials & Interfaces* 13, 49027 – 49042.
27. B. Srinivasan, R. Gautier, F. Gucci, B. Fontaine, J.-F. Halet, F. Cheviré, C. Boussard-Plédel, M.J. Reece, B. Bureau (2018). Impact of coinage metal insertion on the thermoelectric

properties of GeTe solid-state solutions, *The Journal of Physical Chemistry C,* 122, 227 – 235.

28. Z. Dashevsky, I. Horichok, M. Maksymuk, A.R. Muchtar, B. Srinivasan, T. Mori (2022). Feasibility of high performance in *p*-type $Ge_{1-x}Bi_xTe$ materials for thermoelectric modules, *Journal of the American Ceramic Society*, 105, 4500 – 4511.
29. T. Parashchuk, B. Wiendlocha, O. Cherniushok, K. Pryga, K. Ciesielski, E. Toberer, K.T. Wojciechowski (2024). Multiple defect states engineering towards high thermoelectric performance in GeTe-based materials, *Chemical Engineering Journal* 499, 156250.
30. T. Parashchuk, O. Kostyuk, L. Nykyruy, Z. Dashevsky (2020). High thermoelectric performance of p-type $Bi_{0.5}Sb_{1.5}Te_3$ films on flexible substrate, *Materials Chemistry and Physics* 253, 123427.
31. B. Dzundza, L. Nykyruy, T. Parashchuk, E. Ivakin, Y. Yavorsky, L. Chernyak, Z. Dashevsky (2020). Transport and thermoelectric performance of *n*-type PbTe films, *Physica B* 588, 412178.
32. B.S. Dzundza, O.B. Kostyuk, U.M. Pysklynets, Z.M. Dashevsky (2023), Development of high-precision hardware and software tools for automated determination of the characteristics of thermoelectric devices, *J. Physics and Chemistry of Solid State* 24, 278.
33. Z. Dashevsky, S. Shusterman, M. Dariel, I. Drabkin (2002), Thermoelectric efficiency in graded indium-doped PbTe crystals, Journal of Applied Physics, 92,1425 – 1430.
34. J.P. Heremans, B. Wiendlocha, A.M. Chamoire (2012). Resonant levels in bulk thermoelectric semiconductors, Energy & Environmental Science, 5, 5510 – 5530.
35. A. Bali, R. Chetty, A. Sharma, G. Rogl, P. Heinrich, S. Suwas, D.K. Misra, P. Rogl, E. Bauer, R.C. Mallik (2016). Thermoelectric properties of In and I doped PbTe, *Journal of Applied Physics*, 120, 175101.
36. A. Faghri (2014). Heat pipes: review, opportunities and challenges, *Frontiers in Heat Pipes (FHP*) 5.
37. W. Xie, Y. Dai, R. Wang, K. Sumathy (2011). Concentrated solar energy applications using Fresnel lenses: A review, *Renewable and Sustainable Energy Reviews* 15, 2588.
38. A. Pfahl, J. Coventry, M. Röger, F. Wolfertstetter, J.F. Vásquez-Arango, F. Gross, M. Arjomandi, P. Schwarzbözl, M. Geiger, P. Liedke (2017). Progress in heliostat development*, Solar Energy*, 152, 3 – 37.
39. L. Li, X. Gao, G. Zhang, W. Xie, F. Wang, W. Yao (2019). Combined solar concentration and carbon nanotube absorber for high performance solar thermoelectric generators, *Energy Conversion and Management* 183, 109.
40. H.K. Raut, V.A. Ganesh, A.S. Nair, S. Ramakrishna (2011). Anti-reflective coatings: A critical, in-depth review, *Energy & Environmental Science* 4, 3779.
41. A.P. Raman, M.A. Anoma, L. Zhu, E. Rephaeli, S. Fan (2014). Passive radiative cooling below ambient air temperature under direct sunlight, *Nature*, 515, 540.
42. G.J. Snyder, J.R. Lim, C.K. Huang, and J.P. Fleurial (2003). Thermoelectric microdevice fabricated by a MEMS-like electrochemical process. *Nature materials* 2, 528.
43. M. Takashiri, T. Shirakawa, K. Miyazaki, H. Tsukamoto (2007). Fabrication and characterization by bismuth - telluride - based alloy thin-film thermoelectric generators by

a flash evaporation method. *Sens. Actuators* A 138, 329.
44. J. Kurosaki, A. Yamamoto, S. Tanaka, J. Cannon, K. Miyazaki, and H. Tsukamoto (2009). Fabrication and evaluation of a thermoelectric microdevice on a free-standing substrate, *J. Electron. Mater*. 38, 1326.
45. P. Fan, Z. Zheng, V.Li, G. (2015).Lin.Low-cost flexible thin-film thermoelectric generator on zinc-based thermoelectric material. *Appl. Phys. Let*. 106, 073901.
46. M. Takashiri, T. Shirakawa, K. Miyazaki, and H. Tsukamoto (2007). Fabrication and characterization of bismuth–telluride-based alloy thin-film thermoelectric generators by a flash evaporation method, *Sens. Actuators A Phys*. 138, 329.
47. P. Fan, Z.-H. Zheng, Z.-K. Cai, T.-B Chen, P.-J. Liu, X.-M. Cai, D.-P. Zhang, G.-X. Liang, and J.-T Luo (2013), The high performance of a thin-film thermoelectric generator with heat flow running parallel to film surface, *Appl. Phys. Lett*. 102, 033904.
48. M. Mizoshiri, M. Makami, K. Ozaki, K. Kozayashi.(2012). Thin film thermoelectric Modules for power generation using focused solar light, *J. of Elect. Mat.* 41, 1917.
49. K. Tappura, K. Jaakkola (2018). A Thin film thermoelectric generator for large area applications, *Proceeding* 2, 779.
50. P. Fan, Z. Zheng, Z. Cai, T. Chen, P. Liu (2013). The high performance of a thin-film thermoelectric generator with heat flow running parallel to film surface, *Appl. Phys. Let*. 102, 033904.
51. M. Maksymuk, T. Parashchuk, B. Dzundza, L. Nykyruy, L. Chernyak, Z. Dashevsky (2021) Development of the flexible film thermoelectric microgenerator based on Bi_2Te_3 alloys. *J. Materials Today Energy* 21, 100573.
52. O. Kostyuk, Ya. Yavorsky, B. Dzundza, Z. Dashevsky (2021). Development of thermal detector based on flexible film thermoelectric module. *J. Physics and Chemistry of Solid State*. 22, 45.

Submitted: 30.01.2025

Мамикін С.[1] (https://orcid.org/0000-0002-9427-324X),
Дзундза Б.[2] (https://orcid.org/0000-0002-6657-5347),
Шнек Р.[3] (https://orcid.org/0000-0002-5802-1352),
Вихор Л.[4] (https://orcid.org/0000-0002-8065-0526),
Дашевський З.[3] (https://orcid.org/0000-0001-9268-4873)

[1]Інститут фізики напівпровідників імені В.Є. Лашкарьова НАН України, Київ, 03028, Україна;
[2]Кафедра комп'ютерної техніки, Прикарпатський національний
університет імені Василя Стефаника, Івано-Франківськ, 76000, Україна;
[3]Кафедра матеріалознавства, Університет Бен-Гуріон в Негеві, Беер-Шева, 84105, Ізраїль;
[4]Інститут термоелектрики НАН та МОН України, вул. Науки, 1, Чернівці, 58029, Україна

Розробка сонячних енергетичних систем на основі високоефективних об'ємних і плівкових термоелектричних модулів

Через збільшення попиту на енергію та виснаження природних ресурсів розвиток технологій збору енергії стає дуже важливим Термоелектричні пристрої, засновані на прямому перетворенні тепла в електричну енергію, є невід'ємною частиною економічно ефективних, екологічно чистих і паливозберігаючих джерел енергії для виробництва електроенергії, температурних датчиків і управління тепловим режимом. Висока надійність і тривалий час роботи термоелектричних енергетичних систем зумовлюють їх широке використання в космічній промисловості та газопровідних системах. Розвиток і широке застосування сонячних термоелектричних перетворювачів (генераторів) обмежується в основному відносно низьким ККД термоелектричного перетворення. У цій роботі ми вперше пропонуємо використовувати пряме перетворення сонячної енергії системами на основі високоефективних багатоступінчастих термоелектричних модулів, що працюють в діапазоні температур 300 – 900 К, для створення автономних систем з електричною потужністю до 500 Вт і електричним ККД до 15 %. Крім того, ми розробили плівкові термоелектричні модулі на тонких гнучких підкладках із добротністю, що відповідає об'ємним модулям. Такі плівкові термоелектричні перетворювачі з вихідною напругою в кілька вольт і електричною потужністю в кілька мікроват можуть бути використані в мікросистемах сонячної енергетики.

Ключові слова: сонячна енергія, термоелектричний модуль, добротність, плівковий термоелектричний мікроперетворювач.

Надійшла до редакції: 30.01.2025